Original Article

Can modifying shielding, field of view, and exposure settings make the effective dose of a cone-beam computed tomography comparable to traditional radiographs used for orthodontic diagnosis?

Stephanie Ting[a]; Diana Attaia[b]; K. Brandon Johnson[c]; Samer Shoukry Kossa[d]; Bernard Friedland[e]; Veerasathpurush Allareddy[f]; Mohamed I. Masoud[g]

ABSTRACT

Objectives: To analyze the effect of changes in exposure settings, field of view (FOV), and shielding on radiation to an adult and child phantom from cone-beam computed tomography (CBCT) imaging compared to panoramic and lateral cephalometric radiographs.

Materials and Methods: The effective dose to an adult and child anthropomorphic phantom by the CS 9300 using various scan protocols was recorded. Absorbed radiation was measured with optically stimulated luminescence dosimeters and effective dose calculated using 2007 International Commission on Radiological Protection tissue weighting factors. Scan protocols included different FOVs, voxel sizes, and standard versus low-dose protocols. Radiation shielding was used when it did not interfere with FOV. Panoramic and lateral cephalometric radiographs were taken with the Orthophos SL.

Results: Even with shielding, smaller FOVs, and increased voxel sizes, the effective dose of standard CBCT scans was higher than panoramic and lateral cephalometric radiographs. A shielded limited FOV standard scan combined with a lateral cephalometric radiograph resulted in a lower dose ($P < .001$) than a full FOV standard scan. Low-dose shielded scans resulted in significant dose reductions to the adult ($P < .05$) and child ($P < .001$) phantoms compared to the respective panoramic and lateral cephalometric radiographs combined. Image quality analysis was not possible with radiation equivalent phantoms.

Conclusions: Unlike standard CBCTs, shielded low-dose CBCT protocols in the CS 9300 have lower effective doses than conventional radiographs for adult and child phantoms. If high resolution and cranial base visualization are necessary, combining a shielded LFOV standard exposure with a cephalometric radiograph is recommended. (*Angle Orthod.* 2020;90:655–664.)

KEY WORDS: Cone beam computed tomography; Dosimetry; Diagnostic imaging

INTRODUCTION

The use of cone-beam computed tomography (CBCT) as a diagnostic tool in orthodontics has increased dramatically since it was introduced for imaging of the dentomaxillofacial region 2 decades ago.[1] Traditionally, panoramic and lateral cephalometric radiographs have been the standard for orthodontic records. There are limitations to two-dimensional imaging[2–3]: Data extrapolated from panoramic lateral cephalometric radiographs represent a two-dimension-

[a] Orthodontic Resident, Harvard School of Dental Medicine, Boston, Mass, USA.

[b] Teaching Assistant, Department of Oral and Maxillofacial Radiology, Ain Shams University, Cairo, Egypt.

[c] Assistant Clinical Professor, Department of Diagnostic Sciences, University of North Carolina School of Dentistry, Chapel Hill, N.C., USA.

[d] Assistant Professor, Military Technical College, Cairo, Egypt.

[e] Associate Professor, Department of Oral Medicine, Infection and Immunity, Harvard School of Dental Medicine, Boston, Mass, USA.

[f] Brodie Craniofacial Endowed Chair and Professor, Department of Orthodontics, University of Illinois College of Dentistry, Chicago, Ill, USA.

[g] Assistant Professor, Department of Developmental Biology, Director of Advanced Graduate Education in Orthodontics, Harvard School of Dental Medicine, Boston, Mass, USA.

Corresponding author: Dr Mohamed I. Masoud, Department of Developmental Biology, Harvard School of Dental Medicine, 188 Longwood Ave, Boston, MA 02115

Accepted: February 2020. Submitted: July 2019.
Published Online: May 19, 2020

al reconstruction of a three-dimensional (3D) object. With CBCT imaging, visualization of the craniofacial complex and dentition in 3D is feasible.

Accurate diagnostic records are vital to an orthodontist's ability to properly diagnose and treatment plan cases. The advantages of CBCT imaging are its ability to depict the spatial orientation of teeth and roots and visualize dentoalveolar anomalies or pathology.[4] CBCT imaging can also be used to evaluate the airway, treatment superimpositions, temporomandibular joint (TMJ) anatomy, temporary anchorage device positioning, root positions and length, success of bone grafts in cleft palate cases, and treatment planning for orthognathic surgery.[5,6]

Clinicians must act in the best interest of the patient when deciding which imaging modality should be used. The additional information potentially gained from CBCT imaging should be carefully weighed against the risk of increased radiation exposure. Children are at greater risk than adults because of an increased rate of cellular growth and organ development, resulting in increased radiosensitivity. In addition, they have a longer life span during which radiation-induced cancer may develop.[7] This presents an issue because children comprise a large percentage of orthodontic patients.

Panoramic radiographs are generally not compatible with head and neck shielding. Despite the thyroid being outside the field of view (FOV) of the primary beam of a typical CBCT scan, it is one of the most radiosensitive organs in the region as evidenced by its high contribution to the effective dose calculation.[8] Because of anatomical differences, children have more neck structure exposed to radiation than adults.[9] Thyroid shielding has been found to significantly decrease the dose to the thyroid gland in pediatric CBCT scans.[10,11] Using the eyes as a reference for orthodontic measurements instead of the cranial base has been shown to be valid and reproducible**.** This opens the door to pairing 3D facial images with CBCT images limited to the upper and lower jaws and allows further shielding of the eyes and the head.[12–15]

Various factors, including FOV, exposure time, voltage, amperage, and voxel size, affect the amount of detail that can be viewed on a CBCT.[1] Images taken at a smaller voxel size are considered to be sharper but are associated with higher radiation doses because of the increase in exposure needed to produce an image with a higher signal-to-noise ratio.[1,16] In evaluating fenestrations and dehiscences and measuring alveolar bone height and weight, voxel size was observed to affect the precision of measurements.[17,18] Decreasing voxel sizes to 0.25 mm – 0.2 mm was shown to improve the accuracy of bone height and bone thickness measurements.[18,19] For the majority of orthodontic patients with a healthy periodontium, that level of detail is unnecessary. A low-resolution image provides sufficient information about structures of interest and more detail than two-dimensional radiographs.

Currently, there is ongoing debate about the use of CBCT in orthodontics. Some argue that CBCT can be used as a routine imaging option because more diagnostic information is potentially available. Others believe that CBCT imaging is only justified when there are clear clinical benefits.

The purpose of this study was to evaluate the dose to a child and adult anthropomorphic phantom with radiation shielding using various CBCT scan protocols incorporating different combinations of voxel sizes, FOV, and low-dose modes. The aim was to identify a CBCT protocol with doses comparable with that of panoramic and lateral cephalometric radiographs to allow clinicians the option to use CBCT imaging instead of traditional two-dimensional images.

MATERIALS AND METHODS

Anthropomorphic Phantoms

For this study, two tissue-equivalent anthropomorphic phantoms (ATOM Max, CIRS Inc., Norfolk, Va) were used. Adult dosimetry was acquired using an average adult male phantom (ATOM Max Model 711HN, CIRS Inc.). For child dosimetry, an anthropomorphic phantom simulating the size, body type, and mass of an average 10-year-old child (ATOM Model 706HN, CIRS Inc.) was used. The phantoms were sectioned into 25-mm thick axially oriented slabs with slots accepting dosimeters at anatomical locations of interest. During imaging, the phantoms were oriented with sectioned planes parallel to the floor.

Dosimeters

Dose was recorded using optically stimulated luminescence (OSL) dosimeters (Nanodot, Landauer, Glenwood, Ill). Each dosimeter was encased in a plastic holder measuring approximately 1 mm $\times$ 10 mm $\times$ 10 mm. This plastic case prevented loss of energy and any ambient light from reaching the dosimeter, which disrupts data. A total of 24 sets of dosimeters were used, each corresponding to critical radiosensitive organs or tissues in the head and neck region (Figure 1). Each set of dosimeters was cleared of stored energy using a light-emitting diode light pad for 24 hours prior to baseline reading. Dosimeters were read using a portable reader (MicroStar, Landauer), which was calibrated daily.

Because dosimeters need to absorb a threshold amount of radiation for accuracy, each set of dosimeters was exposed five times to ensure reliable measurements and divided by five to calculate the

OSL Dosimeter #	Phantom Location (Organ / Tissue of Interest)	Level in Phantom
1	Calvarium anterior	2
2	Calvarium left	2
3	Calvarium posterior	2
4	Mid-brain	2
5	Mid-brain	3
6	Pituitary	4
7	Right orbit	4
8	Right lens of eye	4-5
9	Left lens of eye	4-5
10	Right maxillary sinus	5
11	Left nasal airway	5
12	Right parotid	6
13	Left parotid	6
14	Left back of neck	6
15	Right ramus	7
16	Left ramus	7
17	Right submandibular gland	7
18	Left submandibular gland	7
19	Center sublingual gland	7
20	Center C spine	8
21	Thyroid superior (left)	8
22	Thyroid (left)	9
23	Thyroid (right)	9
24	Esophagus	9

Figure 1. Child anthropomorphic phantom displaying numbered sections where OSL dosimeters are located.

average exposure per scan. To make sure the data were reproducible and consistent, scans for each imaging modality were repeated on three separate sets of dosimeters. The average dose and standard deviation of each set of dosimeters were calculated. The effective dose was calculated using the 2007 International Commission on Radiological Protection (ICRP) tissue weighting factors.

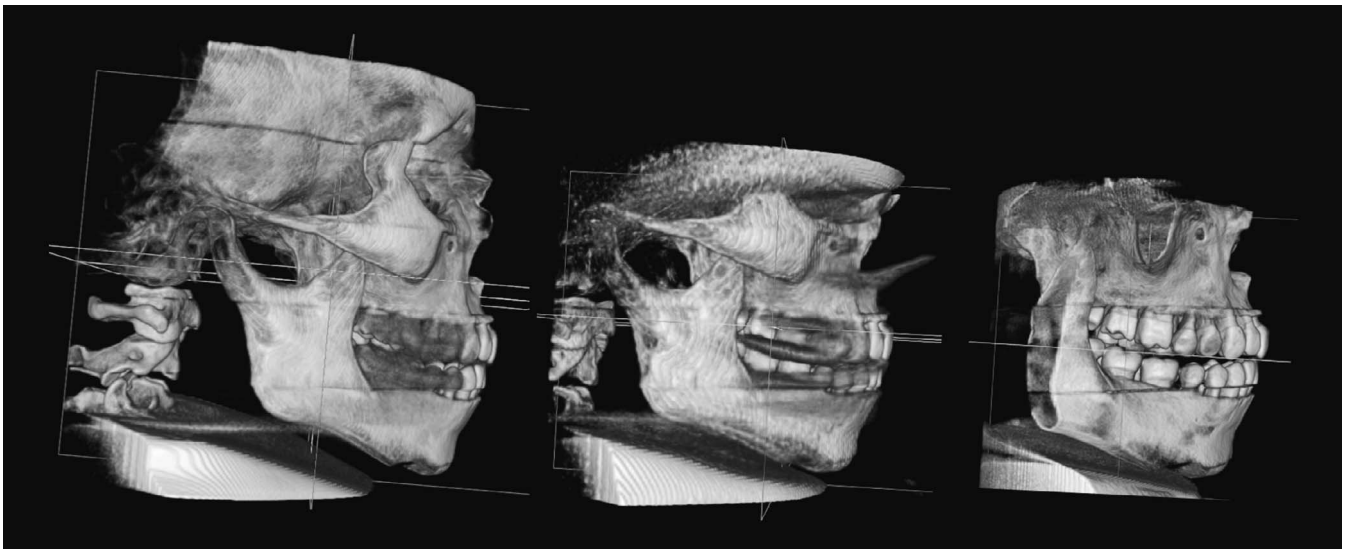

Figure 2. Adult phantom CBCT scout images. FFOV scan at 0.3 voxel standard mode (left), LFOV scan at 0.4 voxel feather mode (middle), and 10×10 cm scan at 0.18 voxel standard mode (right).

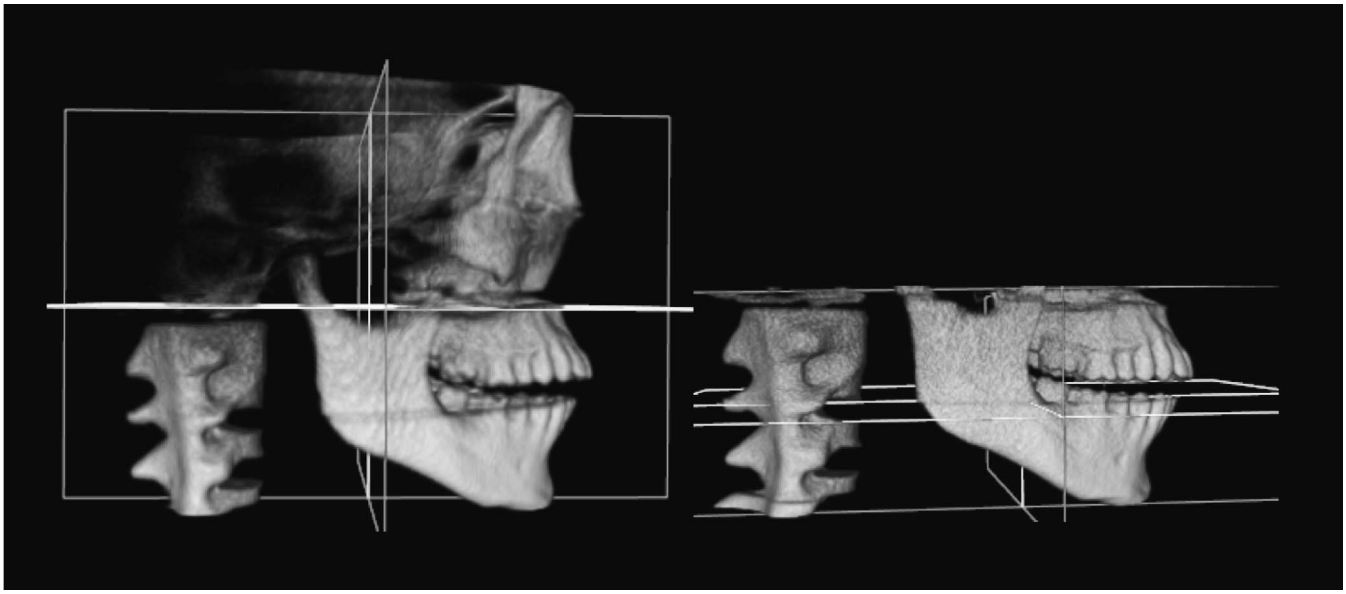

Figure 3. Child phantom CBCT scout images. FFOV scan at 0.4 voxel feather mode (left) and LFOV scan at 0.5 voxel standard mode (right).

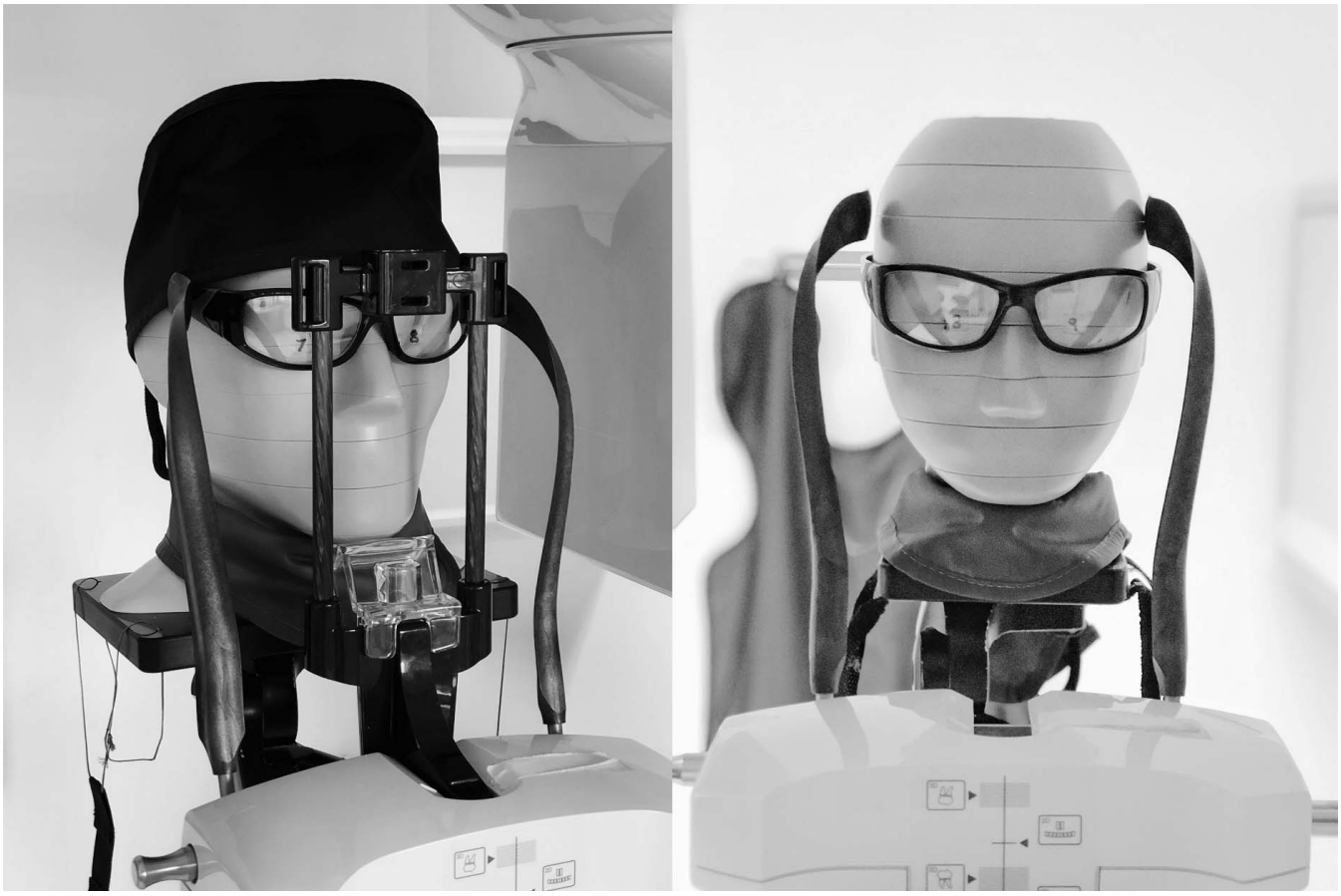

Figure 4. Adult phantom with radiation safety cap, lead glasses, and thyroid collar (left). Child phantom with lead glasses and thyroid collar (right).

Table 1. Scanning Protocols With Settings and Shielding Used for CBCT, Panoramic, and Lateral Cephalometric Radiographs

Phantom	Unit	FOV, cm	Full or Limited Field of View	Protocol	Voxel Size	kVp	mA	Exposure, s	Radiation Shielding
Adult	CS 9300	17 × 13.5	FFOV	Standard	0.3	90	4	11.3	Thyroid collar
Adult	CS 9300	17 × 13.5	FFOV	Standard	0.5	90	4	11.3	Thyroid collar
Adult	CS 9300	17 × 11	LFOV	Standard	0.5	90	4	6.4	Thyroid collar, glasses, radiation cap
Adult	CS 9300	17 × 11	LFOV	Feather	0.4	80	2	3	Thyroid collar, glasses, radiation cap
Adult	CS 9300	10 × 10	LFOV	Standard	0.18	90	4	8	Thyroid collar, glasses, radiation cap
Adult	Orthophos SL			Cephalometric	–	77	14	9.4	Thyroid collar
Adult	Orthophos SL			Panoramic	–	69	12	14	None
Child	CS 9300	17 × 11	FFOV	Standard	0.5	80	4	6.4	Thyroid collar
Child	CS 9300	17 × 11	FFOV	Feather	0.4	70	2	3	Thyroid collar
Child	CS 9300	17 × 6	LFOV	Standard	0.5	80	4	6.3	Thyroid collar, glasses
Child	CS 9300	17 × 6	LFOV	Feather	0.4	70	2	3.7	Thyroid collar, glasses
Child	Orthophos SL			Cephalometric	–	73	15	9.4	Thyroid collar
Child	Orthophos SL			Panoramic	–	63	8	14	None

Imaging and Shielding

To evaluate radiation dose levels, the following CBCT units were utilized: CS 9300 (Carestream Dental, Atlanta, Ga) and Orthophos SL (Sirona, Bensheim, Germany). The anthropomorphic phantoms were centered in the imaging field. A scout image was taken before each type of scan to ensure the phantom was centered and the region of interest was within the FOV. Scout images were taken without OSL dosimeters in place.

CBCT scans were taken at full FOV (FFOV) or limited FOV (LFOV). The FFOV scans incorporated nasion to menton, which measured 17 × 13.5 cm in the adult phantom (Figure 2) and 17 × 11 cm in the child phantom (Figure 3). The LFOV scans incorporated orbitale to menton and measured 17 × 11 cm in the adult phantom (Figure 2) and 17 × 6 cm in the child phantom (Figure 3). In addition, a 10 × 10 cm LFOV scan at a smaller voxel size was performed on the adult phantom to evaluate the dose at a higher resolution voxel setting that would allow more accurate measurements of alveolar bone height and width. The adult and child FFOV scans were performed with a 0.5-mm lead thyroid collar (Model 641CFS, Shielding International, Madras, Ore). The adult LFOV scans were performed with a 0.5-mm lead thyroid collar, 0.75-mm lead radiation safety glasses (Model RG-808, Phillips Safety Products, Middlesex, N.J.), and 0.5-mm lead radiation safety cap (Universal Medical, Norwood, Mass) (Figure 4). The child LFOV scans were performed without the radiation safety cap because it obscured key landmarks as a result of its size on the child phantom.

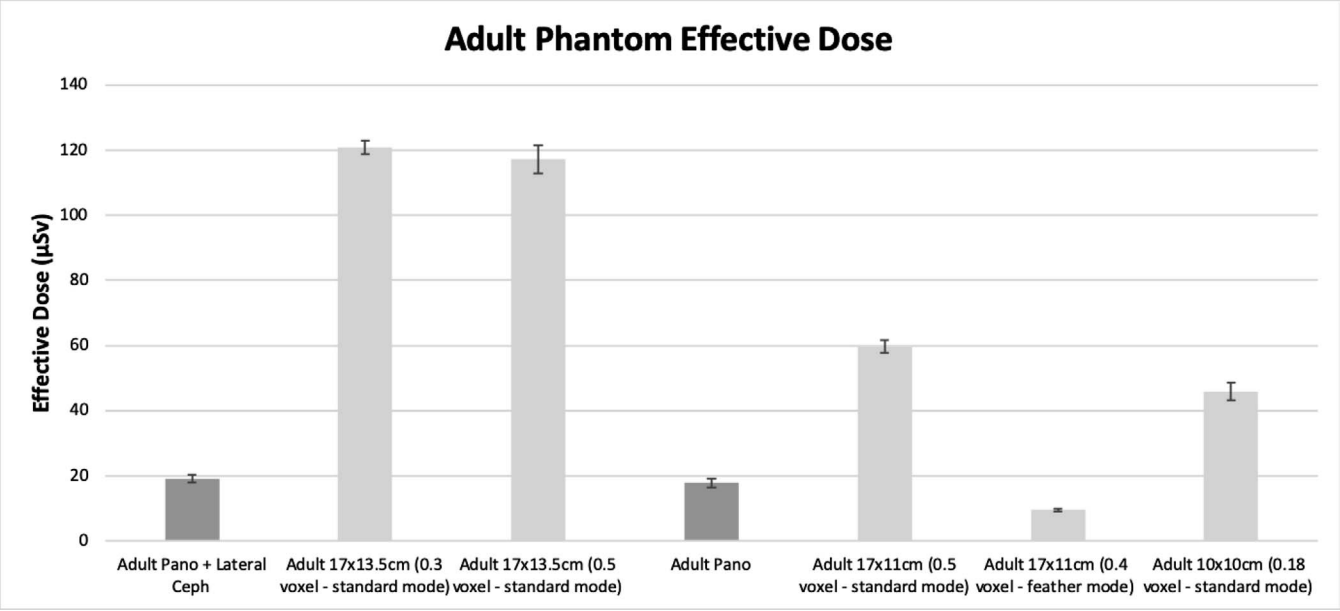

Figure 5. Adult phantom effective dose by scan protocol.

Table 2. Effective Dose (mSv) for Adult Phantom by Scan Protocol[a]

					95% Confidence Interval	
Unit	FOV, cm	Full or Limited Field of View	Voxel	Protocol	Mean Effective Dose, μSv	Effective Dose, μSv: LFOV CBCT + Lateral Ceph
CS 9300	17 × 13.5	FFOV	0.3	Standard	121.03	
CS 9300	17 × 13.5	FFOV	0.5	Standard	117.2	
CS 9300	17 × 11	LFOV	0.5	Standard	60.47	61.77
CS 9300	17 × 11	LFOV	0.4	Feather	9.70	11
CS 9300	10 × 10	LFOV	0.18	Standard	53.49	54.79
Orthophos SL				Pano + Ceph	19.1	
Orthophos SL				Ceph	1.3	
Orthophos SL				Pano	17.8	

[a] Pano, Panoramic; Ceph, Cephalometric; SD, standard deviation; SEM, standard error of the mean; Min, minimum; Max, maximum; HS, highly significant; S, significant.

The low-dose protocol ("feather mode") is a specialized setting on the CS 9300 unit marketed to produce high-quality 3D images at the same or lower dose than a panoramic radiograph. This is achieved by decreasing the peak kilovoltage (kVp), milliamperage (mA), and exposure time. The feather mode protocol was only available for scans at specific FOVs and was not an available setting for the adult FFOV (17 × 13.5 cm) scan.

Panoramic and lateral cephalometric radiographs were taken with the Orthophos SL unit. Manufacturer-recommended settings for an average adult and child were used. Cephalometric radiographs were taken with a 0.5-mm lead thyroid collar. Panoramic radiographs were taken without the thyroid collar as scatter interferes with the diagnostic quality of the images. The scan parameters used for adult and child phantoms are listed in Table 1.

Effective Dose Calculation

The effective dose (E), expressed in microsieverts (μSv), was calculated using the formula: $E = \sum W_T \times H_T$. W_T represents the defined 2007 ICRP tissue weighting factors, which is a measure of the contribution of the specific organ or tissue to the overall health risk. H_T represents the equivalent dose absorbed by the tissue.

Statistical Analysis

Quantitative variables were described by the mean, standard deviation, range (minimum – maximum), standard error, and 95% confidence interval of the mean. One-way analysis of variance was applied for comparing the group's means, whereas for multiple comparisons, the Bonferroni method was applied.

Significance level was considered at $P < .05$; $P < .01$ was considered highly significant. Two-tailed tests were assumed throughout the analysis for all statistical tests.

RESULTS

The mean effective doses are listed for the shielded adult phantom (Table 2) and shielded child phantom (Table 3). The mean effective dose and standard deviation for the adult phantom are depicted in Figure 5 and for the child phantom in Figure 6. The effective dose of the FFOV scans are compared with the dose of the panoramic and lateral cephalometric radiographs

Table 3. Effective Dose (μSv) for Child Phantom by Scan Protocol[a]

					95% Confidence Interval	
Unit	FOV, cm	Full or Limited Field of View	Voxel	Protocol	Mean Effective Dose, μSv	Effective Dose, μSv: LFOV CBCT + Lateral Ceph
CS 9300	17 × 11	FFOV	0.5	Standard	65.17	
CS 9300	17 × 11	FFOV	0.4	Feather	10.13	
CS 9300	17 × 6	LFOV	0.5	Standard	51.3	53.37
CS 9300	17 × 6	LFOV	0.4	Feather	9.17	11.24
Orthophos SL				Pano + Ceph	31.37	
Orthophos SL				Ceph	2.07	
Orthophos SL				Pano	29.3	

[a] Pano, Panoramic; Ceph, Cephalometric; SD, standard deviation; SEM, standard error of the mean; Min, minimum; Max, maximum; HS, highly significant; S, significant.

Table 2. Extended

	95% Confidence Interval							
Dose as Multiple of Pano + Ceph	SD	SEM	Lower Bound	Upper Bound	Min	Max	*P* Value (Compared to Effective Dose of Pano + Ceph)	Statistical Significance
6.33	2.08	1.2	115.87	126.2	119.5	123.4	<.001	HS
6.14	4.25	2.45	106.65	127.75	112.3	119.8	<.001	HS
3.3	1.7	0.98	57.53	66	59.8	62.8	<.001	HS
0.64	0.2	0.12	10.5	11.5	10.8	11.2	<.05	S
2.94	3.46	2	46.19	63.39	50.82	57.16	<.001	HS
1	1.3	0.75	15.87	22.33	17.6	19.9		
0.07	0.1							
0.93	1.39							

combined. The effective dose of the LFOV scans are compared with the dose of the panoramic radiograph.

All doses in standard CBCT scans for the adult and child phantoms were significantly higher ($P < .001$) than the respective doses from panoramic and lateral cephalometric radiographs combined. When comparing scans in standard mode, decreasing the FOV and associated increased shielding resulted in decreased doses to the phantoms. Comparing standard mode CBCT protocols (Figure 7), the shielded LFOV scan combined with a lateral cephalometric radiograph resulted in significantly lower doses ($P < .001$) to both the adult and child phantoms than the FFOV scan.

In low-dose feather mode, the LFOV CBCT combined with a lateral cephalometric radiograph resulted in significantly lower doses to the adult ($P < .05$) and the child ($P < .001$) phantoms than the respective panoramic and lateral cephalometric radiographs. The child FFOV feather mode scan resulted in significantly lower doses ($P < .001$) than the child panoramic and lateral cephalometric radiographs combined.

A high level of reproducibility was found in the CBCT scans and panoramic and lateral cephalometric radiographs as evidenced by similar doses between different trials. The shielded adult low-dose LFOV scan resulted in 36% less radiation than the adult panoramic and lateral cephalometric radiographs. The shielded child low-dose FFOV scan resulted in 68% less radiation than the child panoramic and lateral cephalometric radiographs combined.

DISCUSSION

The aim of this study was to evaluate the effective dose from CBCT imaging compared with conventional panoramic and lateral cephalometric radiographs. Using a combination of shielding, changes in voxel sizes, and FOVs, the goal was to establish a protocol that yielded doses similar to the panoramic and lateral cephalometric radiographs.

The effective doses obtained showed that standard CBCT imaging still imparted higher doses of radiation than conventional orthodontic radiographs, even with shielding. FFOV scans incorporating nasion to menton and TMJ in the adult and child phantoms were tested. The effective dose of a FFOV CBCT in standard mode was more than six times higher in the adult phantom and more than two times higher in the child phantom than doses in the respective panoramic and lateral cephalometric radiographs combined.

Table 3. Extended

	95% Confidence Interval							
Dose as a Multiple of Pano + Ceph	SD	SEM	Lower Bound	Upper Bound	Min	Max	*P* Value (Compared to Effective Dose of Pano + Ceph)	Statistical Significance
2.08	1.53	0.88	61.36	68.97	63.4	66	<.001	HS
0.32	0.5	0.29	8.88	11.38	9.6	11	<.001	HS
1.7	0.21	0.12	52.85	53.88	53.2	54	<.001	HS
0.36	0.15	0.09	10.85	11.61	11.1	11	<.001	HS
1	2.34	1.35	25.54	37.19	28.7	33		
0.07	0.06							
0.93	2.36							

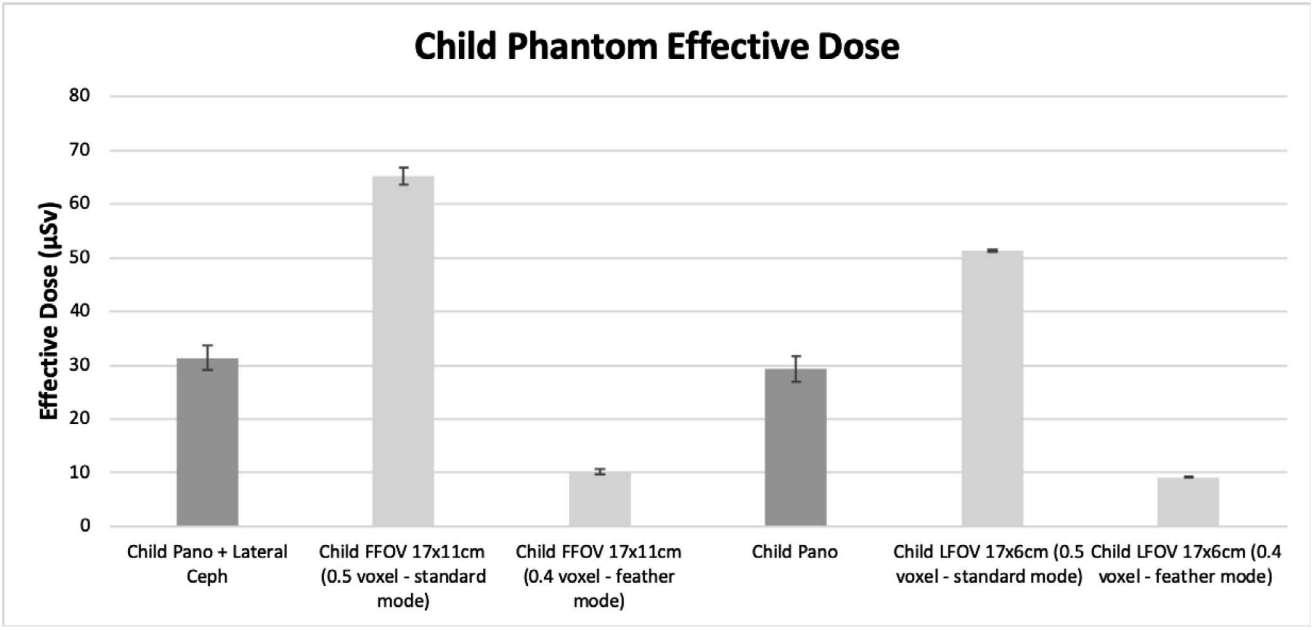

Figure 6. Child phantom effective dose by scan protocol.

Because decreasing FOV lowers dose, LFOV scans incorporating orbitale to menton and TMJ were tested. The LFOV scan combined with a lateral cephalometric radiograph can replicate information obtained from conventional orthodontic radiographs. In addition, the eyes and true horizontal can be used instead of the cranial base as a reference point in cephalometric analysis, making it possible to diagnose the relation-

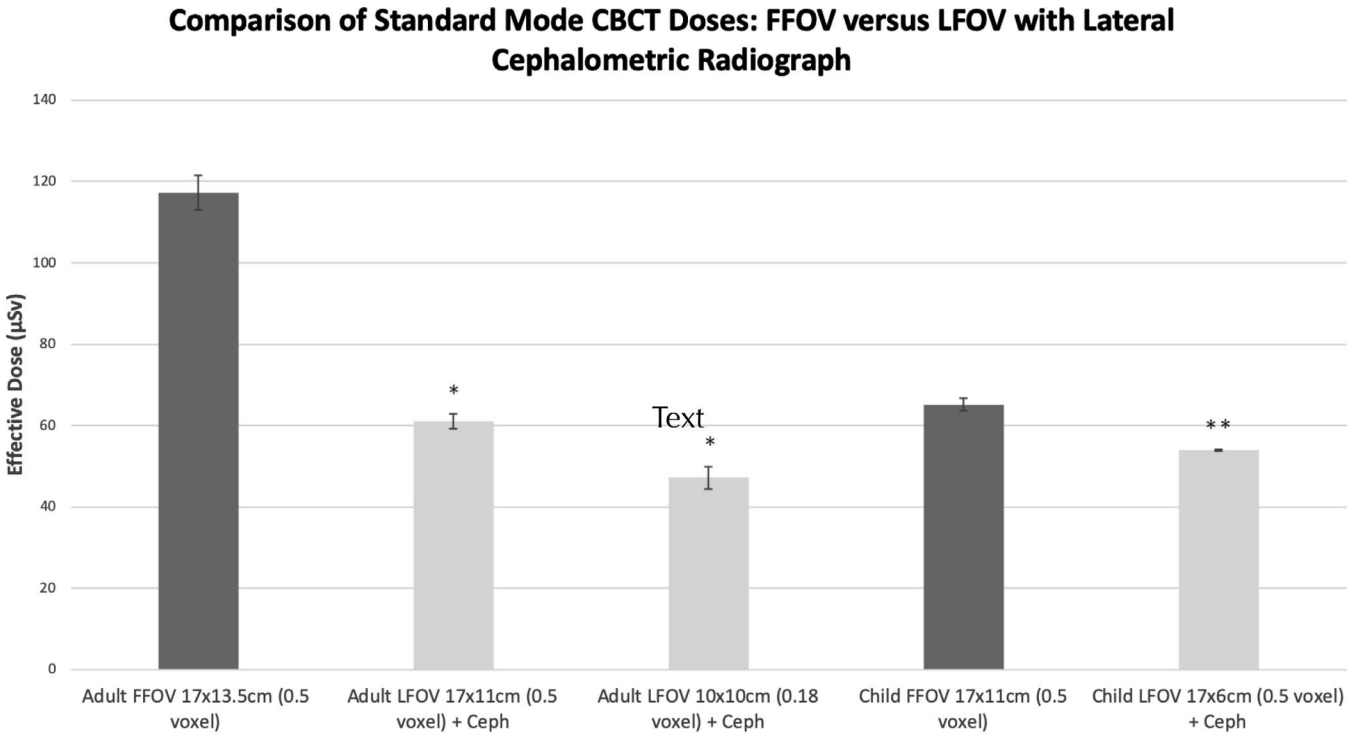

* Highly significant (P<0.001) compared to adult FFOV 17x13.5cm (0.5 voxel)

* * Highly significant (P<0.001) compared to child FFOV 17x11cm (0.5 voxel)

Figure 7. Comparison of effective dose in FFOV scans and LFOV scans combined with a lateral cephalometric radiograph.

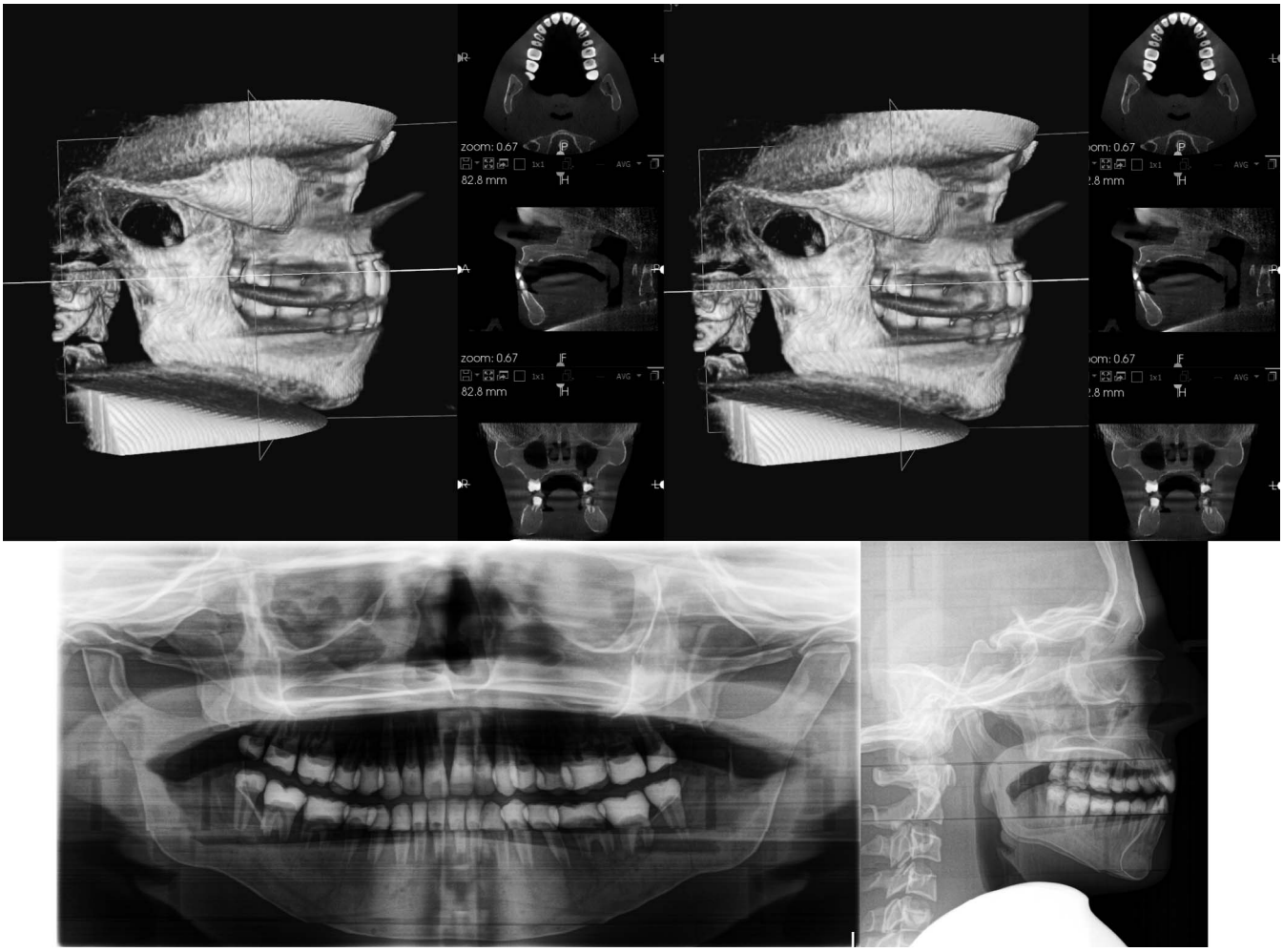

Figure 8. Adult LFOV 0.4 voxel feather mode (top left), adult LFOV 0.5 voxel standard mode (top right), adult panoramic radiograph (bottom left), and adult lateral cephalometric radiograph (bottom right).

ship of the jaws and teeth with just a radiograph localized to the upper and lower jaws superimposed on photographic images of the whole face.[14]

Even with shielding, the effective dose of LFOV scans for the adult and child phantoms in standard mode were significantly higher than the dose of panoramic radiographs. However, a shielded LFOV scan combined with a lateral cephalometric radiograph yielded significantly lower doses ($P < .001$) than the FFOV scan in both the adult and child phantoms. Limiting the FOV on a CBCT scan allows for increased radiation shielding. If the clinician deems a high-resolution CBCT and cranial base visualization to be necessary for treatment planning, a shielded LFOV scan combined with a lateral cephalometric radiograph resulted in less radiation exposure than a FFOV scan.

A notable finding from the study was the significant dose reduction when using the low-dose mode (feather mode) on the CS 9300 unit. In the adult phantom, a shielded LFOV scan in low-dose mode resulted in a 36% dose reduction compared with a traditional adult panoramic radiograph. In the child phantom, the shielded FFOV scan in low-dose mode resulted in a 68% reduction in the effective dose compared with the child panoramic and lateral cephalometric radiographs combined.

The results from this study corroborated data obtained from the Ludlow and Walker[16] study that tested the QuickScan+ protocol on the i-CAT FLX (Imaging Science International, Hatfield, PA). For an adult phantom, a 16 × 11 cm scan using the QuickScan+ protocol on the i-CAT FLX produced an effective dose of 8.8 μSv.[16] In the current study, in an adult 17 × 11 cm scan using feather mode on the CS 9300, the measured effective dose was 9.7 μSv. Both scans using low-dose protocols resulted in effective doses lower than an adult panoramic radiograph, which was measured at 17.8 μSv. This number correlated with data from other studies placing the effective dose of a panoramic radiograph between 14.2

and 24.3 μSv.[20] Similar dose reductions were found for the low-dose CBCT scans in the child phantom.

The use of CBCT as a standard imaging tool in orthodontics has been a source of controversy. Although 3D imaging is a valuable tool, there are concerns about exposure to unnecessary radiation. The balance between increased diagnostic information from CBCT imaging and the risks of increased radiation exposure must be carefully weighed. There has been a recent shift from the principle of "as low as reasonably achievable" to "as low as diagnostically acceptable" to emphasize the importance of prudence when ordering imaging.[21,22]

CBCT imaging using low-dose protocols presents an interesting option for orthodontists. Figure 8 shows an adult LFOV low-dose scan compared with an adult LFOV standard scan and panoramic and lateral cephalometric radiographs. This study was done using radiation-equivalent phantoms, and as a result it was not possible to assess the images for their adequacy for clinical use. However, visual examination of the images indicated that low-dose scans provided similar diagnostic information as conventional orthodontic radiographs in 3D with less radiation exposure.

CONCLUSIONS

- Even with radiation shielding, decreased FOV, and increased voxel sizes, standard CBCT imaging still exposes patients to more radiation than conventional orthodontic radiographs.
- Low-dose (feather mode) shielded CBCT protocols in the CS 9300 resulted in lower effective doses than panoramic radiographs for adult and child phantoms. Low-dose scans can provide useful diagnostic information in most orthodontic patients, but further image quality studies are recommended.
- In cases where higher resolution and cranial base visualization are necessary, combining a shielded LFOV scan and a lateral cephalometric radiograph is recommended.

REFERENCES

1. Hatcher DC. Operational principles for cone-beam computed tomography. *J Am Dent Assoc*. 2010;141:3–6.
2. Moyers RE, Bookstein FL. The inappropriateness of conventional cephalometrics. *Am J Orthod*. 1979;75:599–617.
3. Johnston LE Jr. A few comments on an elegant answer in search of useful questions. *Semin Orthod*. 2011;17:13–14.
4. Hodges RJ, Atchison KA, White SC. Impact of cone-beam computed tomography on orthodontic diagnosis and treatment planning. *Am J Orthod Denotfacial Orthop*. 2013;143: 665–674.
5. Mah JK, Huang JC, Choo H. Practical applicants of cone-beam computed tomography in orthodontics. *J Am Dent Assoc*. 2010;141:7S–13S.
6. Kapila S, Conley RS, Harrell WE Jr. The current status of cone beam computed tomography imaging in orthodontics. *Dentomaxillofac Radiol*. 2011;40:24–34.
7. Kutanzi K, Lumen A, Koturbash I, Miousse I. Pediatric exposures to ionizing radiation: carcinogenic considerations. *Int. J. Environ. Res. Public Health*. 2015;13:1057.
8. International Commission on Radiological Protection. The 2007 recommendations of the International Commission on Radiological Protection. ICRP publication 103. *Ann ICRP*2007;37:1–332.
9. Hujoel P. Thyroid shields and neck exposures in cephalometric radiography. *BMC Med Imag*. 2006; 6: 6
10. Hidalgo A, Davies J, Horner K, Theodoraku C. Effectiveness of thyroid gland shielding in dental CBCT using a paediatric anthropomorphic phantom. *Dentomaxillofac Radiol*. 2015; 44:20140285.
11. Goren AD, Prins RD, Dauer LT, et al. Effect of leaded glasses and thyroid shielding on cone beam CT radiation dose in an adult female phantom. *Dentomaxillofac Radiol*. 2013; 42: 20120260.
12. Masoud MI, Bansal N, Castillo J, et al. 3D dentofacial photogrammetry reference values: a novel approach to orthodontic diagnosis. *Eur J Orthod*. 2017;39(2):215–225.
13. Manosudprasit A, Arsha H, Allareddy V, Masoud MI. Diagnosis and treatment planning of orthodontic patients with 3-dimensional dentofacial records. *Am J Orthod Dentofacial Orthop*. 2017;151(6):1083–1091.
14. Finn SC, Silver MT, Canary B, et al. A modified Steiner's analysis that does not require radiographic exposure of the cranial base. *Orthod Craniofac Res*. 2019;22:1–8.
15. Castillo JG, Azer D, Manosudprasit A, et al. The relationship between 3D dentofacial photogrammetry measurements and traditional cephalometrics measurements on a group of orthodontic patients. *Angle Orthod*. 2019;89:275–283.
16. Ludlow JB, Walker C. Assessment of phantom dosimetry and image quality of i-CAT FLX cone-beam computed tomography. *Am J Orthod Dentofacial Orthop*. 2013;144: 802–817.
17. Sun Z, Smith T, Kortam S, Kim DG, Tee BC, Fields H. Effect of bone thickness on alveolar bone-height measurements from cone-beam computed tomography images. *Am J Orthod Dentofacial Orthop*. 2011;139:e117–e127.
18. Patcas R, Muller L, Ullrich O, Peltomaki T. Accuracy of cone-beam computed tomography at different resolutions assessed on the bony covering of the mandibular anterior teeth. *Am J Orthod Dentofacial Orthop*. 2012;141:41–50.
19. Wood R, Sun Z, Chaudry J, et al. Factors affecting the accuracy of buccal alveolar bone height measurements from cone-bean computed tomography images. *Am J Orthod Dentofacial Orthop*. 2013;143:353–363.
20. Ludlow JB, Davies-Ludlow LE, White SC. Patient risk related to common dental radiographic examinations: the impact of 2007 International Commission on Radiological Protection recommendations regarding dose calculation. *J Am Dent Assoc*. 2008;139:1237–1243.
21. NCRP: achievements of the past 50 years and addressing the needs of the future. Available at: https://ncrponline.org/wp-content/uploads/2018/08/Annual/pp50.pdf; last accessed 9/13/2019.
22. Jaju PP, Jaju SP. Cone-beam computed tomography: time to move from ALARA to ALADA. *Imaging Sci Dent*. 2015;45: 263–265.